Ceramics International xxx (xxxx) xxx–xxx

Contents lists available at ScienceDirect

Ceramics International

journal homepage: www.elsevier.com/locate/ceramint

Sintering behaviour and properties of manganese-doped alumina

S.B. Dhuban[a], S. Ramesh[a,*], C.Y. Tan[a], Y.H. Wong[a], U. Johnson Alengaram[b], S. Ramesh[c], W.D. Teng[d], F. Tarlochan[e], U. Sutharsini[f]

[a] Center of Advanced Manufacturing and Material Processing, Department of Mechanical Engineering, Faculty of Engineering, University of Malaya, 50603 Kuala Lumpur, Malaysia
[b] Centre for Innovative Construction Technology (CICT), Department of Civil Engineering, Faculty of Engineering, University of Malaya, 50603 Kuala Lumpur, Malaysia
[c] Centre for Ionics University of Malaya, Department of Physics, Faculty of Science, University of Malaya, 50603 Kuala Lumpur, Malaysia
[d] Ceramics Technology Group, SIRIM Berhad, Shah Alam 40911, Malaysia
[e] Department of Mechanical and Industrial Engineering, College of Engineering, Qatar University, Doha, Qatar
[f] Department of Physics, University of Jaffna, Jaffna, JA 40000, Sri Lanka

ARTICLE INFO

Keywords:
Alumina
Sintering additive
Manganese doping
Microwave sintering
Conventional sintering

ABSTRACT

The effect of manganese (0.1, 0.5 and 1.0 wt%) on the sintering and mechanical properties of alumina was studied. Sintering was carried out by the conventional heating method in a box furnace and in a hybrid multimode microwave furnace. XRD analysis revealed the precipitation of a spinel second phase ($MnAl_2O_4$) in manganese-doped samples as a result of manganese limited solubility in the corundum lattice. The addition of 0.1 wt% manganese was most beneficial in enhancing the densification of alumina (97.5% relative density when compared to 94.2% for the undoped sample), hindered grain growth, and improved the hardness of the ceramic when sintered at 1500 °C. The study also revealed that microwave sintering was effective in suppressing grain growth of alumina. In addition, the hardness was dependent on the sintered bulk density and that grain coarsening ensued as the density of the sintered alumina exceeded 95% of theoretical.

1. Introduction

Alumina ceramic find its way to numerous technological applications due to its high hardness, deformation resistance, refractoriness, good thermal stability and excellent corrosion resistance [1]. Alumina is also used in several high-tech applications where other materials would fail such as nozzles and linings for refining vessels [2–4]. However, obtaining a fully dense alumina using the conventional pressureless sintering technique requires high sintering temperatures, typically above 1500 °C [5].

In general, it is well documented that the common approach to improve the sintering kinetics and reduce the sintering temperature is to engineer the particle size to be in the nanoscale region. Nano-sized powders are expected to accelerate the densification kinetics and lower the sintering temperature according to Herring's scaling law [6]. This, however requires the use of special chemical processing methods and careful control over the various processing parameters. The other approach which is more economical would be to use dopants or sintering additives to accelerate the densification kinetics in solids through the creation of defects and formation of liquid phase that facilitates particle rearrangement during sintering [7].

Sintering additives have been employed in the sintering of alumina, in particular, magnesium oxide (MgO) is the most studied additive [8–12]. On the other hand, manganese oxide (MnO_2) has been successful in promoting densification for many ceramics including zirconia [13–15], ceria [16–18] and hydroxyapatite [19,20]. Li et al. [21] reported that the addition of manganese to yttria-stabilized zirconia (YSZ) reduced the densification temperature by 200 °C when compared to the undoped YSZ. The authors attributed the improved densification observed for the manganese-doped zirconia to the increased in grain boundary mobility. This increase in grain boundary mobility was explained by the change in the valence state of manganese at high temperatures and the consequent charge unbalancing and oxygen vacancies generation caused by manganese reduction [21–23]. Keski and Cutler [24,25] showed that the densification rate of alumina improved by manganese addition up to 0.3%. Other studies found that high concentration of MnO_2 (3.0 wt%) enhanced the densification and the hardness of alumina [26,27].

Microwave sintering has been widely studied as a rapid heating technique that offers many benefits over conventional sintering method [28]. Brosnan et al. [29] studied the effect of microwave on the densification of alumina and showed that a 95% dense alumina was

* Corresponding author.
E-mail address: ramesh79@um.edu.my (S. Ramesh).

https://doi.org/10.1016/j.ceramint.2018.12.207
Received 14 December 2018; Received in revised form 28 December 2018; Accepted 28 December 2018

obtained after microwave sintering at 1350 °C as compared to 1600 °C for conventionally heated samples. Zuo et al. [30] investigated the effects of MgO doping on the microwave sintering of alumina and they found that dopant played a role in enhancing the microwave effect thus promoting densification.

On the other hand, Żymełka et al. [31] found that microwave had no effect on the densification of undoped alumina, but microwaves induced palpable effect on the densification of MgO-doped alumina [31,32]. Croquesel et al. [33] reported that microwave enhanced the sintering process during the initial and intermediate stage of densification but this enhancement diminishes as the density increased and levels off at around 95% of theoretical density. Moreover, alumina powder with low specific surface area value densified better using conventional sintering than microwave sintering. Xie et al. [34] also found that the microwave-enhanced densification was significant at the early stages of sintering, but this enhancement diminished as samples approached theoretical density.

In this study, the effect of low additions of MnO_2 as a sintering additives on the densification and mechanical properties of alumina were investigated. Comparison was made using both the conventional and microwave sintering methods.

2. Materials and methods

Commercially available 99.9% pure Al_2O_3 (Kyoritsu, Japan) and MnO_2 (BDH) powders were used as the starting materials. The alumina powder was mixed with various percentages (0.1, 0.5 and 1.0 wt%) of MnO_2 by attrition milling. The wet mixture was homogenised for 30 min at 600 rpm using the attritor mill (Union Process, USA), with zirconia balls and ethanol as a milling medium. The mixture was filtered and the slurry was dried in an oven at 60 °C for 24 h. The dried powder was then sieved through 212 µm sieve to obtain soft, free flowing powder. Green samples in the form of a disk (20 mm in diameter) were uniaxial pressed and subjected to cold isostatic pressing at 200 MPa prior to sintering.

Conventional sintering (CS) was carried out in air at four different temperatures i.e. 1300, 1400, 1500 and 1600 °C. The heating and cooling rate applied was 10 °C/min with 2 h dwell time. For comparison purpose, hybrid microwave sintering (MS) was also carried out at 1500 °C in a 2.45 GHz, 6 kW multimode microwave furnace to evaluate the efficacy of MW in retarding grain coarsening of alumina.

Sintered compacts were ground using different grades (rough to fine) of SiC papers and subsequently polished using 6 µm and 1 µm diamond paste to obtain a reflective surface. Phase analysis was performed using X-Ray diffraction (EMPYREAN, PANalytical, Netherlands). The XRD uses Cu-Kα radiation source, operating at 40 kV in step mode with 0.02° 2θ step and a count time of 0.5 s per step. XRD was performed over a 2θ range from 20° to 60°. Prior to microstructure analysis, sintered compacts were thermally etched at 50 °C lower than their corresponding sintering temperatures with 30 min dwell time. Microstructural analysis was done using a scanning electron microscope (SEM). Images were taken at randomly selected spots throughout the samples (edge and center) from which the average grain size was determined in accordance to the line intercept method [35]. Bulk density was measured according to the water immersion method based on Archimedes principle. The theoretical density of alumina was taken as 3.98 g cm^{-3} [36]. Vickers hardness of the polished samples was determined using Vickers hardness tester (Mitutoyo AVK-C2, Japan) at an indentation load of 10 kgf and loading time of 10 s.

3. Results and discussion

The XRD phase analysis conducted on all the Mn-doped Al_2O_3, regardless of sintering conditions, revealed the presences of mainly the corundum alumina phase with minute $MnAl_2O_4$ spinel being detected as the second phase, as typically shown in Fig. 1. The presences of this

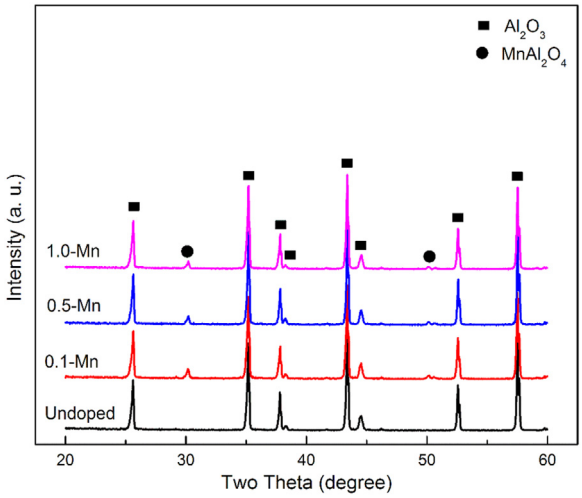

Fig. 1. Typical XRD patterns of undoped and manganese-doped alumina sintered at 1600 °C.

second phase indicates a limited solubility of manganese in alumina. The valence difference between manganese and alumina may lead to vacancies or interstitials creation in the corundum lattice [37] and this may have an effect on the mechanical properties of the ceramic.

The effect of dopants and sintering temperatures on the relative density of alumina is presented in Fig. 2. At low sintering temperature of 1300 °C, the undoped alumina densified better than the Mn-doped alumina, with 0.1 wt% Mn-doped samples achieving lowest relative density of about 64%. This observation was supported by the microstructural development which revealed higher porosity than other samples when sintered at the same temperature, see Fig. 3e, where densification process was still at the early stage and only necking between the particles are visible without grain boundaries.

As the sintering temperature increased to 1400 °C, the densification rate of Mn-doped Al_2O_3 sample increased and surpassed the density of undoped sample. At this temperature, samples containing higher manganese content (0.5 and 1.0 wt%) exhibited improved densification. The 1 wt% Mn-doped sample developed distinct and clear grain boundaries (Fig. 3n) in comparison to other samples. Nevertheless, sintering at 1500 °C resulted in all Mn-doped samples achieving higher relative densities than the undoped sample. The Mn-doped alumina recorded relative densities of above 97%, while undoped samples recorded a relative density of 94%. The microstructure of the Mn-doped samples sintered at 1500 °C (Fig. 3g, k and o) revealed almost complete densification with some intergranular and intergranular closed pores being visible while the undoped alumina (Fig. 3c) exhibited open pores.

At 1600 °C, the densification rate of the 1 wt% Mn-doped samples

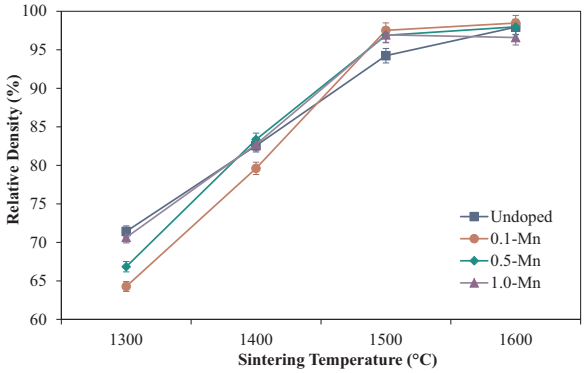

Fig. 2. Effect of sintering temperature and manganese doping on the relative density of conventional-sintered alumina.

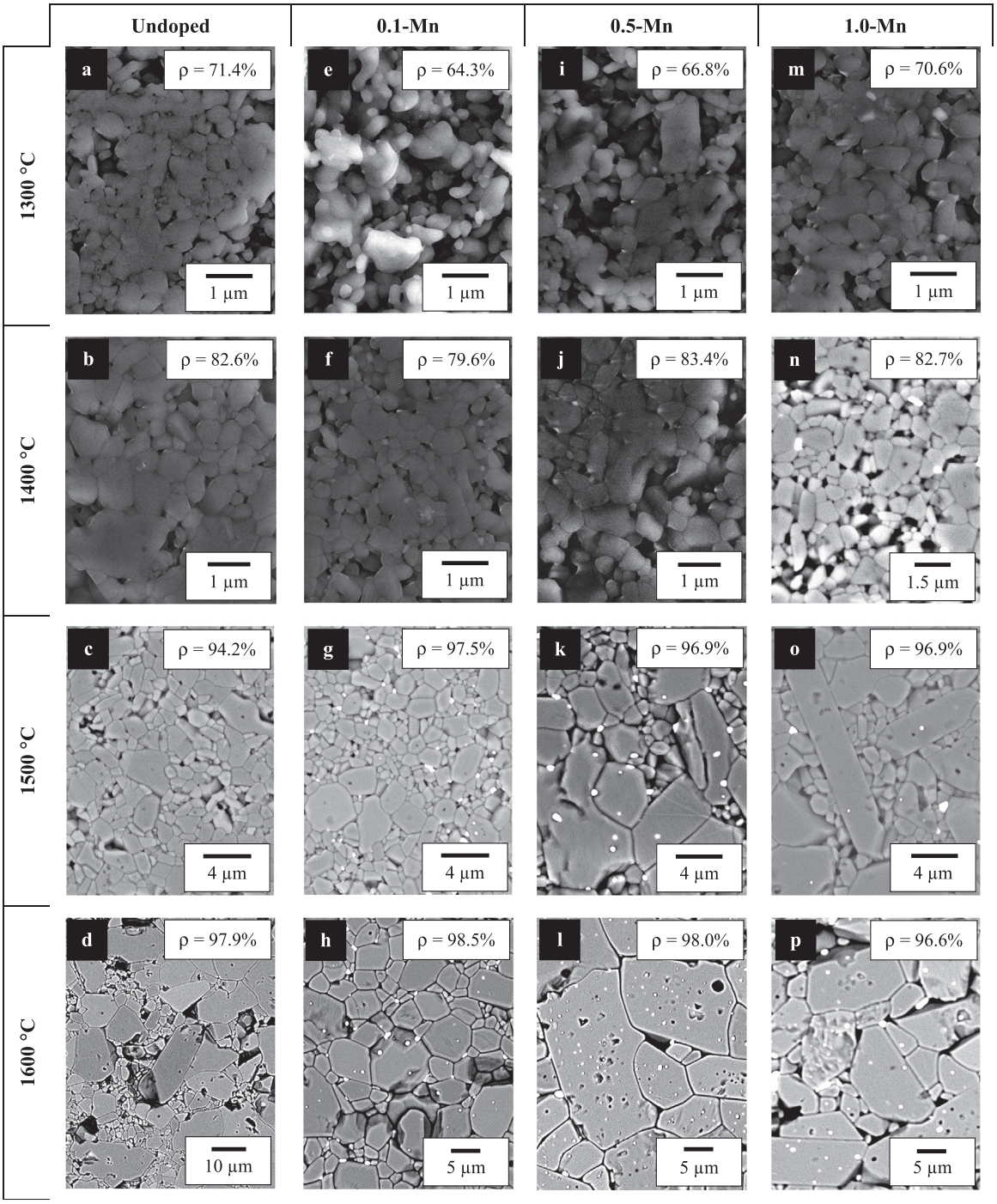

Fig. 3. Microstructural evolution of undoped and manganese-doped samples sintered at various temperatures. The relative density (ρ) for the sample is as stated in the SEM micrograph.

was slightly lower than other samples. This lower density noted for this alumina sample correlates well with the observation made for other ceramics when doped with manganese and could be attributed to the evaporation of manganese at high temperatures [21,22,38]. This small variation in the densification of Mn-doped samples and undoped sample sintered at temperatures exceeding 1500 °C was in good agreement with other studies [27,39]. Furthermore, the observed effectiveness of 0.1 wt% manganese addition on the densification of alumina is consistent with the results reported by Keski and Cutler [24,25]. In the present work, the 0.1 wt% Mn-doped samples achieved the highest relative densities (98.5%) of all tested compositions. Undoped samples developed an inhomogeneous microstructure (Fig. 3d), whereas manganese-doped samples developed a more homogeneous microstructures (Fig. 3h, i, and p) at high sintering temperature.

The addition of 0.1 wt% manganese oxide did not only result in enhanced densification but also was effective in suppressing alumina grain growth as depicted in Fig. 4. The 0.1 wt% Mn-doped alumina yielded the lowest average grain size of all tested samples. For example the average grain size of this ceramic was 1.04 μm when sintered at 1500 °C whereas the undoped sample yielded a higher grain size of 1.23 μm. This lower grain size regime of the 0.1 wt% Mn-doped samples is in good agreement with that reported for MgO-doped alumina [32]. At 1500 °C, the 0.5 wt% Mn- and 1.0 wt% Mn-doped alumina showed moderate grain growth with some smaller grains trapped between

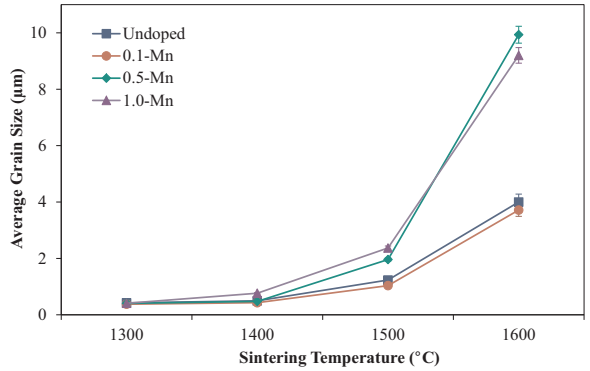

Fig. 4. Effect of sintering temperature on the average grain size of alumina ceramics.

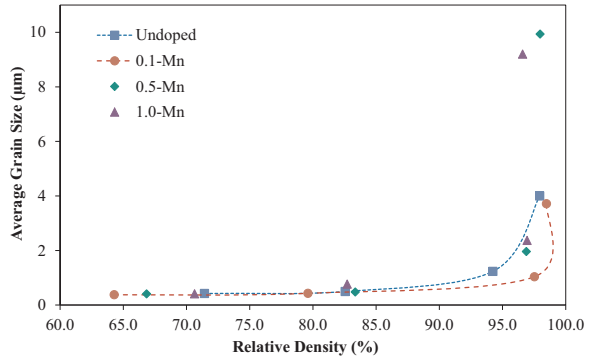

Fig. 5. Average grain size versus relative density trajectory of undoped and manganese-doped alumina. The dotted lines show the trajectory of undoped and 0.1 wt% Mn-doped alumina.

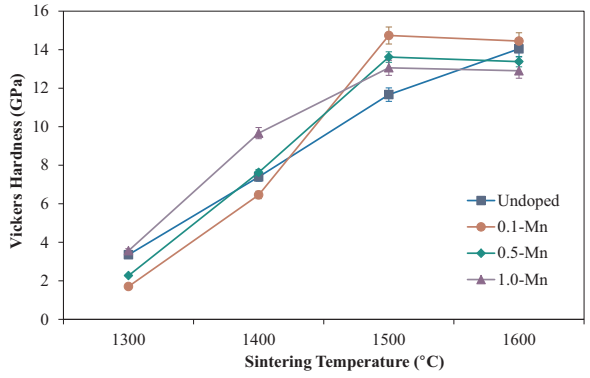

Fig. 6. The effect of sintering temperature and manganese content on the Vickers hardness of conventional-sintered alumina.

larger grains, see Fig. 3k and o. However, abnormal grain growth was observed for the 0.5 wt% Mn- and 1.0 wt% Mn-doped alumina sintered at 1600 °C (Fig. 3l and p). At this temperature, grain growth proceeded particularly in high manganese doped samples resulting in abnormal grain growth with grains as large as 50 μm were observed. In addition, some elongated grains, as long as 20 μm with an aspect ratio of 5 were visible for the 1 wt% Mn-doped alumina when sintered at 1500–1600 °C. This study also found that the grain growth of alumina ensued rapidly in all samples after attaining about 95% relative density as shown in Fig. 5. It was also evident that the addition of 0.1 wt% Mn was beneficial in retarding grain coarsening and enhanced densification of alumina as depicted by the dotted line in Fig. 5. It is envisaged that the manganese could have played a role during sintering by changing its valence state (i.e. reduction from Mn^{4+} to Mn^{2+}) thus creating

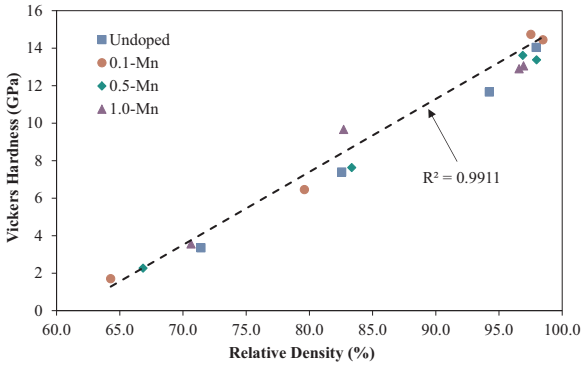

Fig. 7. The variation of Vickers hardness and relative density of alumina, revealing a linear relationship existed between both properties.

Table 1
Properties comparison for alumina ceramics sintered at 1500 °C by conventional sintering (CS) and microwave sintering (MS).

Dopant content (wt%)	Vickers hardness (GPa)		Relative density (%)		Average grain size (μm)	
	CS	MS	CS	MS	CS	MS
Undoped	11.66	8.98	94.2	88.7	1.23	0.72
0.1-Mn	14.74	11.61	97.5	91.2	1.04	0.71
0.5-Mn	13.62	12.24	96.9	92.0	1.96	0.85
1.0-Mn	13.06	12.24	96.9	92.2	2.37	0.95

vacancies or interstitials to maintain electrical neutrality. This in turn could have increased the grain boundary mobility and atomic movements [21,27,37], resulting in fast densification if compared to that of the undoped ceramic.

The effect of dopant addition and sintering temperatures on the hardness of alumina is shown in Fig. 6. The undoped sample showed almost a linear increase in hardness with sintering temperature from 3.3 GPa at 1300 °C to 14 GPa at 1600 °C. On the other hand, the Mn-doped samples exhibited an increasing hardness trend up to 1500 °C and then decreased slightly when sintered at 1600 °C. The hardness of the Mn-doped alumina was higher than the undoped sample when sintered at 1400–1500 °C. At sintering temperature of 1400 °C, although, both undoped and 1.0 wt% Mn-doped samples had similar relative density of about 83%, there is distinct difference in the hardness between the two samples. This indicates that the dopant played a positive role in enhancing the hardness of alumina. At 1500 °C, all manganese-doped samples had significantly higher hardness (> 13 GPa) than undoped alumina (11.6 GPa). In particular, the 0.1 wt% Mn-doped alumina exhibited the highest hardness of 14.7 GPa and this could be associated with the improved densification of the ceramic. However, as the sintering temperature increased to 1600 °C, all the manganese-doped samples showed a slight decrease in the hardness, and this could be attributed to grain coarsening [40,41]. An attempt to correlate the hardness and relative density revealed a linear relationship exist as shown in Fig. 7, thus indicating that the hardness is dependent on the densification of the alumina ceramic.

Comparison of the effect of microwave sintering on the properties of alumina ceramics sintered at 1500 °C is as given in Table 1. In general, the relative density and hardness of the MS samples were slightly lower than the CS samples. However, microwave sintering was beneficial in retarding the grain coarsening of alumina i.e. all the samples had grain sizes of below 1 μm. The comparison of the microstructure evolution of the MS and CS samples are shown in Fig. 8. The CS samples and manganese-doped samples revealed a microstructure with a small number of isolated pores, whereas MS samples exhibited open pores which signifies incomplete densification. At density of about 92% of

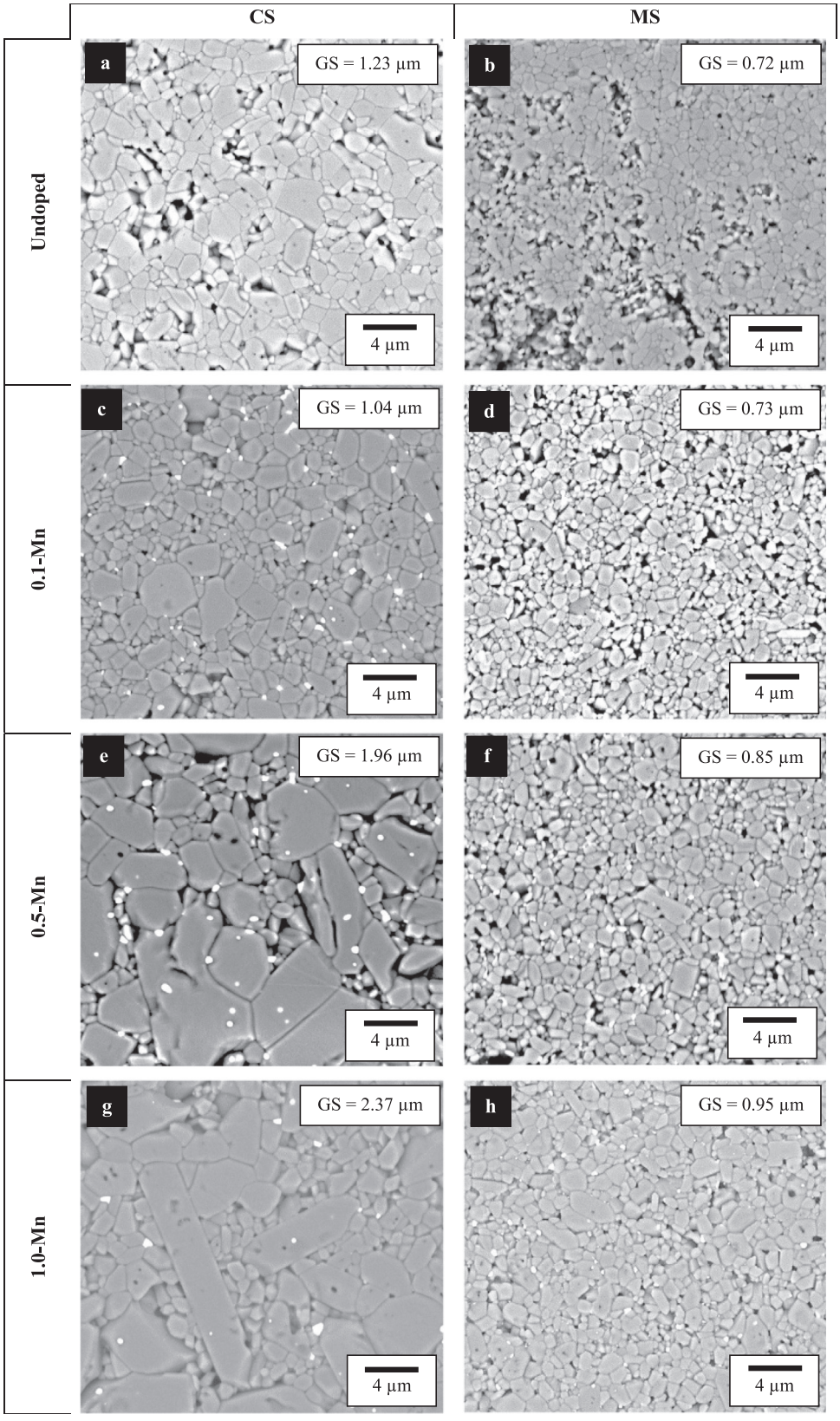

Fig. 8. SEM micrographs comparing the microstructure evolution (1500 °C) between the conventional sintered (CS) and microwave sintered (MS) alumina. The average grain size (GS) of the sample is as shown in the micrograph.

theoretical, MS samples were at the end of the intermediate stage of sintering whereas the CS samples have entered the final stage of sintering.

4. Conclusions

The effect of manganese doping (0.1, 0.5 and 1.0 wt%) and sintering temperatures on the properties of alumina ceramic were studied. In addition, the efficacy of microwave sintering in retarding the grain coarsening of alumina was also evaluated. The XRD analysis revealed the development of minute $MnAl_2O_4$ spinel secondary phase in all the Mn-doped ceramics regardless of sintering methods, thus indicating a limited solubility of manganese in alumina. It was found that 0.1 wt% manganese was most beneficial in enhancing the densification of alumina at 1500 °C with sample recording a relative density of 97.5% and hardness of 14.7 GPa. Furthermore, the 0.1 wt% Mn-doped alumina experienced lower grain growth and resulted in a homogeneous microstructure. In contrast, the addition of 0.5 wt% and 1.0 wt% promoted abnormal grain growth when sintered at 1500–1600 °C. The study also demonstrated that grain coarsening of alumina could be suppressed via microwave sintering i.e. all the samples recorded a grain size of below 1 μm when sintered at 1500 °C without significantly affecting other properties. It was also found that the hardness of alumina varied linearly with relative density and that grain coarsening was inevitable once the density exceeded about 95% of theoretical.

Acknowledgements

The authors gratefully acknowledge University of Malaya, Malaysia for the support rendered in carrying out this research.

References

[1] J. Li, Y. Ye, Densification and grain growth of Al_2O_3 nanoceramics during pressureless sintering, J. Am. Ceram. Soc. 89 (2006) 139–143.
[2] M.D. Innocentini, A.R. Pardo, V.C. Pandolfelli, B.A. Menegazzo, L.R. Bittencourt, R.P. Rettore, Permeability of high-alumina refractory castables based on various hydraulic binders, J. Am. Ceram. Soc. 85 (2002) 1517–1521.
[3] M.M. Dimitrijević, B. Medjo, R.J. Heinemann, M. Rakin, T. Volkov-Husović, Experimental and numerical analysis of thermal shock damages to alumina based ceramic disk samples, Mater. Des. 50 (2013) 1011–1018.
[4] C. Aneziris, F. Homola, D. Borzov, Materials and process development of advanced refractories for innovative metal processing, Adv. Eng. Mater. 6 (2004) 562–568.
[5] H. Li, X. Xi, J. Ma, K. Hua, A. Shui, Low-temperature sintering of coarse alumina powder compact with sufficient mechanical strength, Ceram. Int. 43 (2017) 5108–5114.
[6] C. Herring, Effect of change of scale on sintering phenomena, J. Appl. Phys. 21 (1950) 301–303.
[7] G.J. Pereira, R.H.R. Castro, D.Z. de Florio, E.N.S. Muccillo, D. Gouvêa, Densification and electrical conductivity of fast fired manganese-doped ceria ceramics, Mater. Lett. 59 (2005) 1195–1199.
[8] L. Radonjić, V. Srdić, Effect of magnesia on the densification behavior and grain growth of nucleated gel alumina, Mater. Chem. Phys. 47 (1997) 78–84.
[9] K.A. Berry, M.P. Harmer, Effect of MgO solute on microstructure development in Al_2O_3, J. Am. Ceram. Soc. 69 (1986) 143–149.
[10] D. Galusek, K. Ghillányová, J. Sedláček, J. Kozánková, P. Šajgalík, The influence of additives on microstrucutre of sub-micron alumina ceramics prepared by two-stage sintering, J. Eur. Ceram. Soc. 32 (2012) 1965–1970.
[11] T. Ikegami, N. Iyi, I. Sakaguchi, Influence of magnesia on sintering stress of alumina, Ceram. Int. 36 (2010) 1143–1146.
[12] K. Maca, V. Pouchlý, K. Bodišová, P. Švančárek, D. Galusek, Densification of fine-grained alumina ceramics doped by magnesia, yttria and zirconia evaluated by two different sintering models, J. Eur. Ceram. Soc. 34 (2014) 4363–4372.
[13] S. Ramesh, S. Meenaloshini, C.Y. Tan, W.J.K. Chew, W.D. Teng, Effect of manganese oxide on the sintered properties and low temperature degradation of Y-TZP ceramics, Ceram. Int. 34 (2008) 1603–1608.
[14] T.S. Zhang, Z.H. Du, S. Li, L.B. Kong, X.C. Song, J. Lu, J. Ma, Transitional metal-doped 8 mol% yttria-stabilized zirconia electrolytes, Solid State Ion. 180 (2009) 1311–1317.
[15] G. Clavel, M.-G. Willinger, D. Zitoun, N. Pinna, Manganese-doped zirconia nanocrystals, Eur. J. Inorg. Chem. 2008 (2008) 863–868.
[16] L. Wu, J.A. Aguiar, P.P. Dholabhai, T. Holesinger, T. Aoki, B.P. Uberuaga, R.H.R. Castro, Interface energies of nanocrystalline doped ceria: effects of manganese segregation, J. Phys. Chem. C. 119 (2015) 27855–27864.
[17] L. Wu, S. Dey, M. Gong, F. Liu, R.H.R. Castro, Surface segregation on manganese doped ceria nanoparticles and relationship with nanostability, J. Phys. Chem. C. 118 (2014) 30187–30196.
[18] T. Zhang, L. Kong, Z. Zeng, H. Huang, P. Hing, Z. Xia, J. Kilner, Sintering behavior and ionic conductivity of $Ce_{0.8}Gd_{0.2}O_{1.9}$ with a small amount of MnO_2 doping, J. Solid State Electrochem. 7 (2003) 348–354.
[19] S. Ramesh, C.Y. Tan, C.L. Peralta, W.D. Teng, The effect of manganese oxide on the sinterability of hydroxyapatite, Sci. Technol. Adv. Mater. 8 (2016) 257–263.
[20] I. Sopyan, S. Ramesh, N.A. Nawawi, A. Tampieri, S. Sprio, Effects of manganese doping on properties of sol–gel derived biphasic calcium phosphate ceramics, Ceram. Int. 37 (2011) 3703–3715.
[21] H. Li, F.L. Souza, R.H.R. Castro, Kinetic and thermodynamic effects of manganese as a densification aid in yttria-stabilized zirconia, J. Eur. Ceram. Soc. 38 (2018) 1750–1759.
[22] C.-H. Chang, J.F. Rufner, K.V. Benthem, R.H. Castro, Design of desintering in tin dioxide nanoparticles, Chem. Mater. 25 (2013) 4262–4268.
[23] S. Dey, J. Mardinly, Y. Wang, J.A. Valdez, T.G. Holesinger, B.P. Uberuaga, J.J. Ditto, J.W. Drazin, R.H. Castro, Irradiation-induced grain growth and defect evolution in nanocrystalline zirconia with doped grain boundaries, Phys. Chem. 18 (2016) 16921–16929.
[24] J.R. Keski, I.B. Cutler, Effect of manganese oxide on sintering of alumina, J. Am. Ceram. Soc. 48 (1965) 653–654.
[25] J. Keski, I. Cutler, Initial sintering of Mn_xO-Al_2O_3, J. Am. Ceram. Soc. 51 (1968) 440–444.
[26] H. Erkalfa, Z. Misirli, T. Baykara, Densification of alumina at 1250 °C with MnO_2 and TiO_2 additives, Ceram. Int. 21 (1995) 345–348.
[27] H. Erkalfa, Z. Misirli, M. Demirci, C. Toy, T. Baykara, The densification and microstructural development of Al_2O_3 with manganese oxide addition, J. Eur. Ceram. Soc. 15 (1995) 165–171.
[28] M. Oghbaei, O. Mirzaee, Microwave versus conventional sintering: a review of fundamentals, advantages and applications, J. Alloy Comp. 494 (2010) 175–189.
[29] K.H. Brosnan, G.L. Messing, D.K. Agrawal, Microwave sintering of alumina at 2.45 GHz, J. Am. Ceram. Soc. 86 (2003) 1307–1312.
[30] F. Zuo, C. Carry, S. Saunier, S. Marinel, D. Goeuriot, R. Bordia, Comparison of the microwave and conventional sintering of alumina: effect of MgO doping and particle size, J. Am. Ceram. Soc. 96 (2013) 1732–1737.
[31] D. Żymełka, S. Saunier, D. Goeuriot, J. Molimard, Densification and thermal gradient evolution of alumina during microwave sintering at 2.45 GHz, Ceram. Int. 39 (2013) 3269–3277.
[32] F. Zuo, S. Saunier, S. Marinel, P. Chanin-Lambert, N. Peillon, D. Goeuriot, Investigation of the mechanism(s) controlling microwave sintering of α-alumina: influence of the powder parameters on the grain growth, thermodynamics and densification kinetics, J. Eur. Ceram. Soc. 35 (2015) 959–970.
[33] J. Croquesel, D. Bouvard, J.-M. Chaix, C.P. Carry, S. Saunier, S. Marinel, Direct microwave sintering of pure alumina in a single mode cavity: grain size and phase transformation effects, Acta Mater. 116 (2016) 53–62.
[34] Z. Xie, J. Yang, Y. Huang, Densification and grain growth of alumina by microwave processing, Mater. Lett. 37 (1998) 215–220.
[35] M.I. Mendelson, Average grain size in polycrystalline ceramics, J. Am. Ceram. Soc. 52 (1969) 443–446.
[36] S.K.C. Pillai, B. Baron, M.J. Pomeroy, S. Hampshire, Effect of oxide dopants on densification, microstructure and mechanical properties of alumina-silicon carbide nanocomposite ceramics prepared by pressureless sintering, J. Eur. Ceram. Soc. 24 (2004) 3317–3326.
[37] S.K. Roy, R.L. Coble, Solubilities of magnesia, titania, and magnesium titanate in aluminum oxide, J. Am. Ceram. Soc. 51 (1968) 1–6.
[38] L. Wu, P.P. Dholabhai, B.P. Uberuaga, R.H. Castro, Temperature dependence discontinuity in the stability of manganese-doped ceria nanocrystals, Cryst. Growth Des. 17 (2017) 446–453.
[39] M. Sathiyakumar, F.D. Gnanam, Influence of MnO and TiO_2 additives on density, microstructure and mechanical properties of Al_2O_3, Ceram. Int. 28 (2002) 195–200.
[40] J.A. Wollmershauser, B.N. Feigelson, E.P. Gorzkowski, C.T. Ellis, R. Goswami, S.B. Qadri, J.G. Tischler, F.J. Kub, R.K. Everett, An extended hardness limit in bulk nanoceramics, Acta Mater. 69 (2014) 9–16.
[41] A. Krell, A new look at the influences of load, grain size and grain boundaries on the room temperature hardness of ceramics, Int. J. Ref. Met. Hard Mater. 16 (1998) 331–335.